Journal of Materials Chemistry C

ROYAL SOCIETY OF CHEMISTRY

PAPER

View Article Online
View Journal | View Issue

Cite this: J. Mater. Chem. C, 2026, 14, 2888

Liquid crystal tetramers and spontaneous chirality: the heliconical twist-bend nematic phase

Ewan Forsyth, †[a] Magdalena M. Majewska, [b] Rebecca Walker, *[a] Damian Pociecha, [b] Ewa Gorecka, [b] John M. D. Storey[a] and Corrie T. Imrie ‡[a]

Received 8th September 2025,
Accepted 10th December 2025

DOI: 10.1039/d5tc03351a

rsc.li/materials-c

The synthesis and characterisation of six groups of liquid crystal tetramers that vary in the nature of the flexible spacers are reported. Each group consists of four mesogenic units: two outer cyanobiphenyl fragments and two inner benzylideneaniline units. Three different types of spacers are used to connect these: ether linked, methylene linked, and an alkyloxy chain. In each group of tetramers, the outer spacers are held constant, and the central spacer is varied. All the tetramers reported exhibit a conventional nematic, N, phase. The nematic–isotropic transition temperature, T_{NI}, and associated entropy change $\Delta S_{NI}/R$ are dependent on the parity of the central spacer but not as strongly as seen in liquid crystal dimers, indicating that the four mesogenic units are not strongly orientationally correlated along the molecular length. Values of $\Delta S_{NI}/R$ shown by tetramer series CB7O.O*m*O.O7CB and CB7O.*n*.O7CB are remarkably large, almost without precedence for low mass mesogens. In addition to the N phase, tetramers with two odd-membered outer spacers exhibit a twist-bend nematic, N_{TB}, phase whereas those having two even-membered outer spacers show a smectic A phase, revealing that the length and parity of the spacer mostly determine phase behaviour. A compound with an odd-membered methylene-linked central spacer is a single exception to this behaviour and this is attributed to the highly bent nature of the central spacer. A surprising inversion is seen in the sense of the odd–even effect associated with the N_{TB}–N transition temperature on switching an ether linked to a methylene linked central spacer. This is attributed to differences in the interaction strength between the unlike mesogenic groups.

Introduction

The origin of homochirality in biological systems remains one of the most significant questions in science and although many different mechanisms have been proposed, a common first step involves spontaneous mirror symmetry breaking.[1] In this context, the discovery of the twist-bend nematic, N_{TB}, phase is of very significant fundamental interest as the first example of mirror symmetry breaking in a fluid with no positional order and consisting of achiral molecules.[2–4] In a conventional nematic, N, phase, the long axes of the rod-like molecules lie more or less in the same direction, known as the director, whereas their centres of mass are randomly distributed, and the phase is fluid. Dozov predicted that bent molecules should exhibit variants of the conventional N phase including the N_{TB} phase.[5] At the heart of Dozov's seminal work is the assertion that bent molecules have a strong natural tendency to pack into bent structures. Arrangements based on pure uniform bend deformation of the director field, however, cannot fill space, and so apart from the bend, the director of such a phase must also experience either splay or twist deformation. In the case of twist, this gives rise to the N_{TB} phase in which the director forms a heliconical structure, being on average tilted with respect to the helical axis. Chirality is formed spontaneously in the N_{TB} phase and an equal number of doubly degenerate left- and right-handed helices would be expected to form. This degeneracy is removed for chiral molecules and the chiral N^*_{TB} phase is obtained.[6,7] A striking feature of the N_{TB} phase is that the pitch length of the helix is remarkably short and typically just a few molecular lengths. Dozov also predicted the existence of twist-bend smectic phases and these have also been discovered.[8–10]

The molecular requirement for the observation of the N_{TB} phase is a bent molecular shape and this has most commonly been realised using odd-membered liquid crystal dimers (see, for recent examples,[11–24]). A mesogenic dimer consists of two mesogenic units connected by a flexible spacer, normally an

[a] Department of Chemistry, School of Natural and Computing Sciences, University of Aberdeen, Old Aberdeen, AB24 3UE, UK. E-mail: rebecca.walker@abdn.ac.uk
[b] Faculty of Chemistry, University of Warsaw, 02-089, ul. Zwirki i Wigury 101, Warsaw, Poland
† Present address: Department of Chemistry, University of Oxford, South Parks Road, Oxford, OX1 3PS, UK.
‡ Deceased January 2025.

alkyl chain,[25,26] and the phase behaviour of such molecules is strongly dependent on the length and parity of the spacer. In essence, the parity of the spacer controls the molecular shape, and in general, dimers containing an odd-membered spacer are bent, and those with an even-membered spacer are linear although exceptions have been reported.[27] The properties of higher liquid crystal oligomers such as trimers consisting of molecules containing three mesogenic units and two flexible spacers,[28–30] and tetramers having four mesogenic units and three flexible spacers[31–35] also depend strongly on the length and parity of the spacers. An odd-membered spacer gives a bent molecular fragment and an even-membered spacer a linear fragment, and the overall molecular shape will depend on the number and placement of these fragments in the oligomer. Very few higher oligomers have been shown to exhibit the N_{TB} phase.[36–48] It appears, however, that the properties of the N_{TB} phase shown by these higher oligomers differ from those of the N_{TB} phase comprised of dimers; for example, the pitch length of the N_{TB} phase and its temperature dependence are very different for dimers than for trimers and tetramers.[36,40] The physical significance of this observation, or indeed its generality, is far from clear. Exploring this observation is not only of considerable fundamental importance in developing our understanding of spontaneous mirror symmetry breaking in these materials, but also it has been shown that the heliconical N_{TB} phase has very significant application potential[49–53] and this structural modification provides a versatile means by which we may tailor the properties of the N_{TB} phase for specific applications.

To further establish and better understand the relationship between the molecular structure of liquid crystal higher oligomers and the formation of the N_{TB} phase, here we report the behaviour of a range of new tetramers (Fig. 1). These consist of outer cyanobiphenyl and inner benzylideneaniline-based mesogenic units. Ether or methylene links are used to connect the spacers and mesogenic units, and different combinations of odd and even-membered spacers have been studied. Varying these structural elements allows for the shape of the molecule to be varied, and hence, furthers our understanding of how the shape affects the phase behaviour in tetramers. The acronyms used to refer to the tetramers are also shown in Fig. 1.

Experimental

Synthesis

An overview of the synthetic routes used to obtain the target tetramers is shown in Scheme 1. Final products were obtained by the condensation of either an 1,ω-bis(4-aminophenyl-4′-oxy)-alkane (I-2-*m*), 1-(4-aminophenoxy)-6-(4-aminophenyl)hexane (I-3), or an 1,ω-bis(4-aminophenyl-4′-)alkane (I-4-*n*) with 1-(4-formylphenoxy)-6-(4-cyanobiphenyl-4′-yl)hexane or 1-(4-formylphenoxy)-7-(4-cyanobiphenyl-4′-yl)heptane (I-1-*z*). Detailed descriptions of the synthesis and characterisation of all the final products and their intermediates are provided in the SI.

Thermal characterisation

The phase behaviour of the materials was studied by differential scanning calorimetry performed using a Mettler Toledo DSC3 differential scanning calorimeter equipped with a TSO 801RO sample robot and calibrated using indium and zinc standards. Heating and cooling rates were 10 K min^{-1}, with a 3 min isotherm between positive and negative ramping profiles, and all samples were measured under a nitrogen atmosphere. Transition temperatures and associated enthalpy changes were extracted from heating traces unless otherwise noted. For each sample, two aliquots were measured, and the data listed are the average of the two sets of data.

Optical characterisation

Liquid crystal phases were visualised by polarised light microscopy, using an Olympus BH2 microscope equipped with a Linkam TMS 92 heating stage and a Zeiss AxioImager A2m microscope equipped with a Linkam LTS420 heating stage. Optical birefringence was measured with a setup based on a photoelastic modulator (PEM-90, Hinds) working at a modulation frequency f = 50 kHz; as a light source, a halogen lamp (Hamamatsu LC8) equipped with narrow bandpass filters (633 nm and 690 nm) was used. The signal from a photodiode (FLC Electronics PIN-20) was deconvoluted with a lock-in amplifier (EG&G 7265) into 1f and 2f components to yield a retardation induced by the sample. Knowing the sample thickness, the retardation was recalculated into optical birefringence. Samples were prepared in 4.9-micron-thick cells with planar anchoring. The alignment quality was checked prior to measurement by inspection under the polarised light optical microscope.

Structural characterisation

X-ray diffraction (XRD) measurements were performed with a Bruker D8 GADDS system (CuKα line, Goebel mirror, point beam collimator, Vantec2000 area detector). The temperature of the samples was controlled with a precision of $\pm$0.1 K. Samples were prepared as droplets on a heated surface. AFM measurements were performed using a Bruker Dimension Icon Microscope working in tapping or ScanAsyst mode, and cantilevers with an elastic constant of 0.4 N m^{-1} were applied.

Molecular modelling

The geometric parameters of the tetramers were obtained using quantum mechanical DFT calculations with Gaussian 09 software.[54] Geometry optimisation of the structures was performed using Gaussian G09W at the B3LYP/6-31G(d) level of theory. Visualisations of the space-filling models were produced post-optimisation using the QuteMol package.[55]

Results and discussion

The transitional properties of the five new members of the CB6O.O*m*O.O6CB series reported here are listed in Table 1 along with those of m = 5 and 6 reported previously.[36] All seven

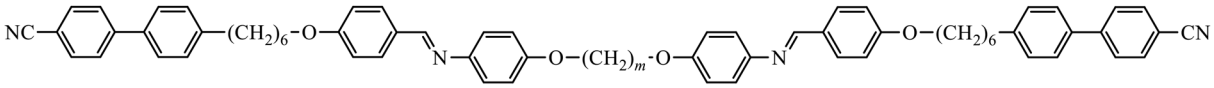

CB6O.O*m*O.O6CB

m = 3-9

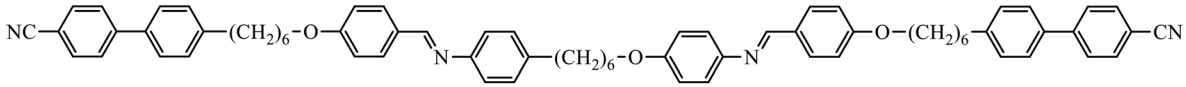

CB6O.6O.O6CB

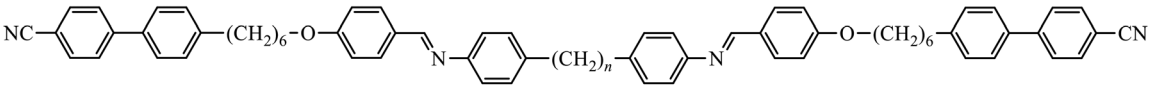

CB6O.*n*.O6CB

n = 7-10

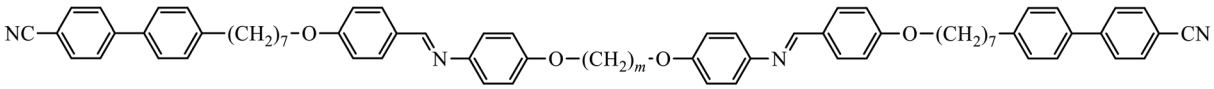

CB7O.O*m*O.O7CB

m = 3-9

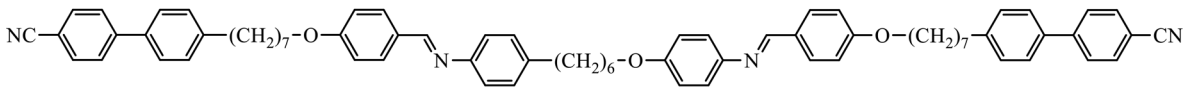

CB7O.6O.O7CB

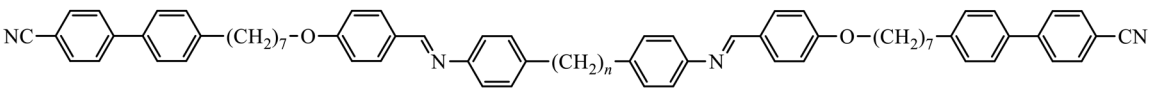

CB7O.*n*.O7CB

n = 7,8

Fig. 1 The structures of the tetramers and the acronyms used to refer to them.

members exhibit an enantiotropic conventional nematic, N, phase identified by the observation of a schlieren optical texture containing both two- and four-brush point singularities, as shown in Fig. 2, and which flashed when subjected to mechanical stress. On cooling the nematic phase of each member, the schlieren texture became rather blocky or developed rope-like or striped regions (Fig. 2) and the optical flickering associated with director fluctuations in the N phase ceased. These changes are characteristic of the formation of the twist-bend nematic, N_{TB}, phase. These phase assignments were supported by X-ray diffraction studies. Specifically, the diffraction patterns obtained for the N and N_{TB} phases were essentially identical containing only diffuse signals in the wide- and small-angle regions indicative of the liquid-like arrangement of

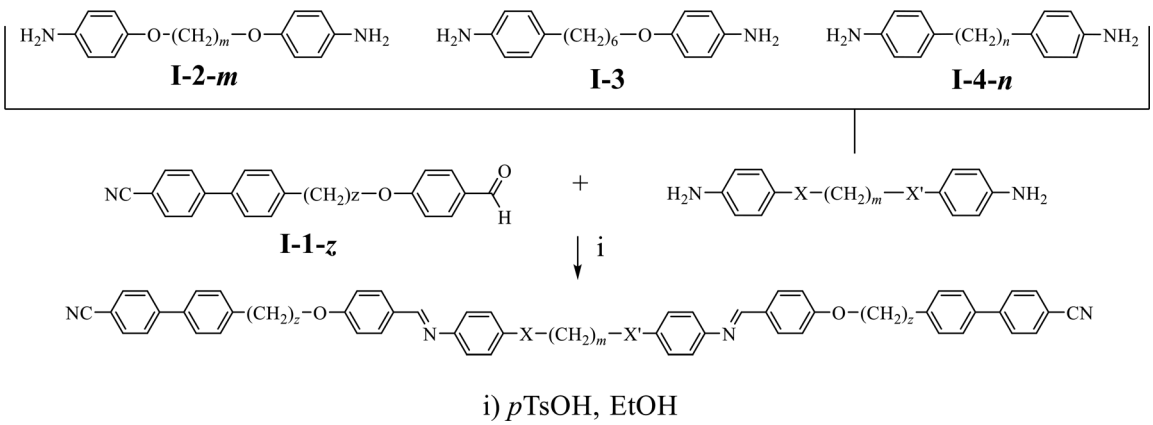

Scheme 1 An overview of the synthesis of the tetramers shown in Fig. 1.

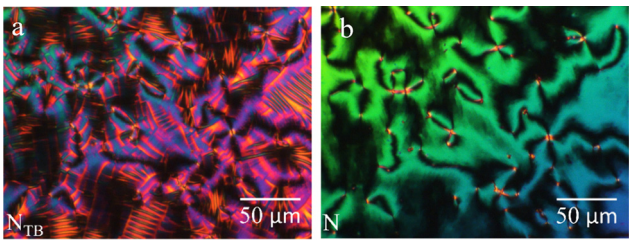

Fig. 2 (a) The striped texture of the twist-bend nematic phase (T = 168 °C) and (b) the schlieren texture of the nematic phase (T = 183 °C) shown by CB6O.O4O.O6CB.

the molecules (Fig. 3). The diffraction signal in the small angle region is very weak in both nematic phases, and its position corresponds to a periodicity of about 12–15 Å, which is related to the length of a single mesogenic unit and suggests a locally intercalated structure. The helical pitch length in the N_{TB} phase shown by CB6O.O5O.O6CB was measured using AFM to be around 30 nm (Fig. 4). This is much larger than the pitch length observed in the N_{TB} phase of liquid crystalline dimers such as CB7CB[4] and CB6OCB.[56] AFM studies of CB6O.O6O.O6CB following rapid cooling to room temperature revealed a pattern consistent with the formation of a lower temperature mesophase below the N_{TB} phase, tentatively assigned as a lamellar phase, in coexistence with the emerging crystal phase, as shown in Fig. 5(a). If the layer planes were parallel to the surface, an additional structure within the layer was evident with a periodicity of around 12 nm (Fig. 5(b)), suggesting a modulated-type smectic phase. Unfortunately, any conclusive identification of this smectic phase using XRD or polarised light microscopy was precluded by the rapid crystallisation of the sample. Measurements of the birefringence for the CB6O.O-mO.O6CB tetramers revealed slightly higher values for even m than for odd (Fig. 6). This reflects the higher orientational order

Table 1 Transition temperatures (°C), and associated scaled entropy changes ($\Delta S/R$) for the CB6O.OmO.O6CB series. [•] indicates a monotropic transition. Data have been extracted from DSC traces measured on heating unless noted otherwise

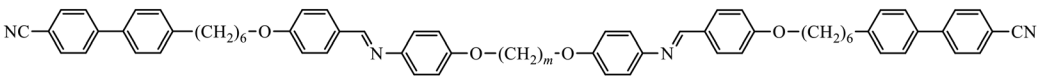

CB6O.OmO.O6CB

m	Cr		N_{TB}		N		I
3	•	158 (11.77)	[•]	157 (0.30)	•	212 (1.32)	•
4	•	164 (17.13)	•	182[b]	•	249 (1.93)	•
5	•	156 (11.44)	•	162 (0.21)	•	215 (1.09)	•
6[c]	•	166 (26.49)	[•]	166[a] (0.04)	•	235 (2.09)	•
7	•	147 (24.13)	•	161 (0.28)	•	209 (1.26)	•
8	•	165 (24.94)	[•]	161[a] (0.02)	•	222 (1.91)	•
9	•	146 (22.82)	•	161 (0.21)	•	205 (1.38)	•

[a] Data extracted from DSC cooling trace. [b] Transition temperature obtained using POM. [c] On cooling, a smectic phase is observed in coexistence with the emerging crystal phase using AFM (see text).

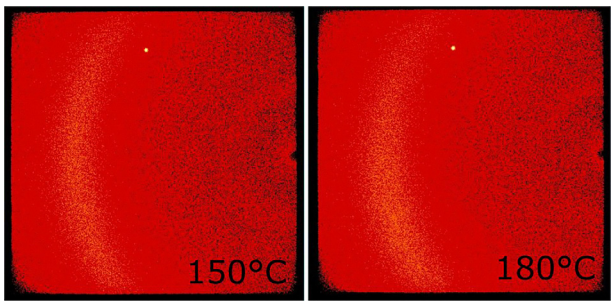

Fig. 3 X-ray diffraction patterns obtained for CB6O.O7O.O6CB at T = 150 °C in the twist-bend nematic phase (left), and at T = 180 °C in the nematic phase (right).

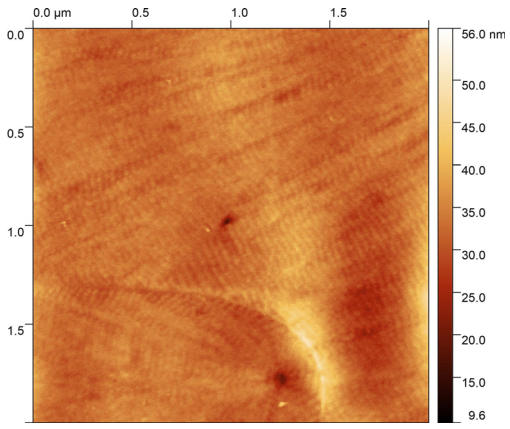

Fig. 4 AFM picture of N_{TB} phase shown by CB6O.O5O.O6CB, and the periodicity of visible stripes is ~30 nm.

for the tetramers having a linear central fragment, and this is also seen in the higher values of $\Delta S_{NI}/R$ for even values of m (Table 1).

The four members of the CB6O.n.O6CB series also exhibit N_{TB} and N phases, and the transitional properties of the new members are listed in Table 2 along with those of CB6O.7.O6CB

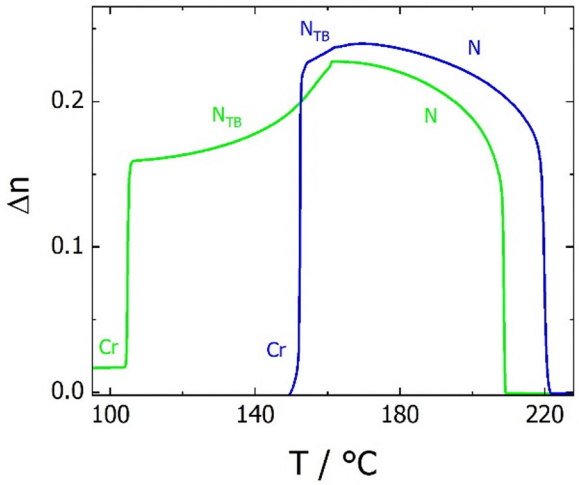

Fig. 6 The temperature dependence of the optical birefringence for CB6O.O7O.O6CB (green line) and CB6O.O8O.O6CB (blue line).

and CB6O.8.O6CB reported previously.[36] The X-ray diffraction patterns obtained for both the N and N_{TB} phases showed only diffuse signals in both the wide and small angle regions (Fig. S2), and the positions of the small angle signals indicated the local intercalated packing of the molecules. The values of the birefringence measured for these tetramers are in general smaller than those seen for the corresponding members of the CB6O.O6O.O6CB series, and again the even members show the higher values (Fig. 7); such an effect has previously been observed in liquid crystal dimers.[57]

The transitional properties of the corresponding tetramers with even-membered outer spacers, the CB7O.OmO.O7CB and CB7O.n.O7CB series, are listed in Tables 3 and 4, respectively. All seven members of the CB7O.OmO.O7CB series show enantiotropic nematic phases, as shown in Fig. 8(a), however, on cooling compounds with m = 3–8 exhibit, instead of N_{TB} phase, a smectic phase. Based on its truncated fan-like texture, as shown in Fig. 8(b–d), the phase is identified as a smectic A phase. The two members of the CB7O.n.O7CB series both show

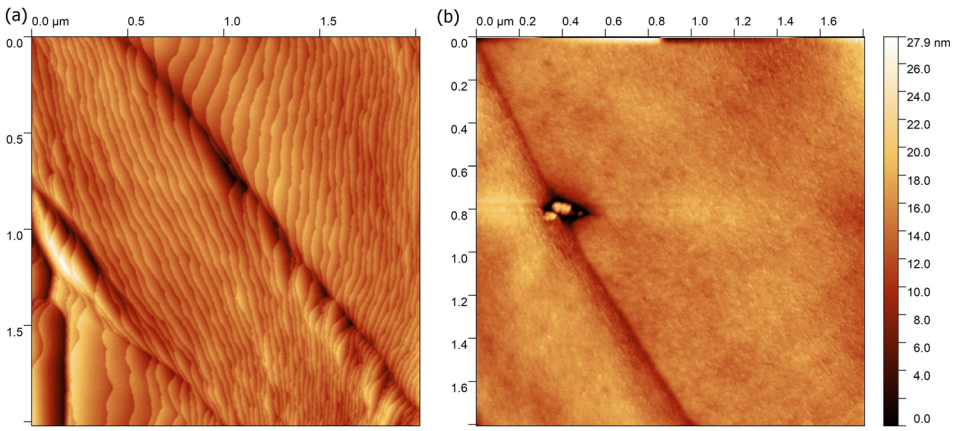

Fig. 5 AFM picture of the smectic phase shown by CB6O.O6O.O6CB. (a) The layers are inclined with respect to the sample surface, and (b) the layers are parallel to the sample surface.

Table 2 Transition temperatures (°C), and associated scaled entropy changes ($\Delta S/R$) for the CB6O.*n*.O6CB series. Data have been extracted from DSC traces obtained on heating

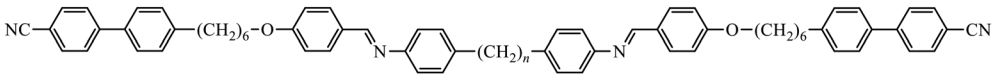

CB6O.*n*.O6CB

n	Cr		N_{TB}		N		I
7	•	140 (8.32)	•	159 (0.84)	•	180 (0.81)	•
8	•	131 (13.01)	•	152 (0.02)	•	212 (2.81)	•
9	•	114 (11.65)	•	157 (0.78)	•	179 (0.91)	•
10	•	128 (23.44)	•	144 (0.02)	•	200 (2.80)	•

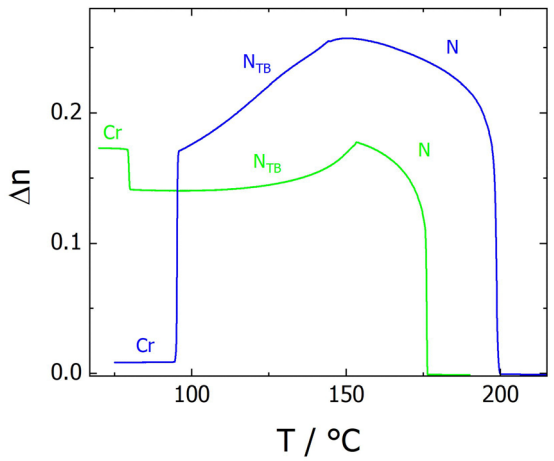

Fig. 7 The temperature dependence of the optical birefringence for CB6O.9.O6CB (green line) and CB6O.10.O6CB (blue line).

an enantiotropic N phase, as shown in Fig. 9 and 10. On cooling the nematic phase shown by n = 7, an N_{TB} phase is formed,[36] whereas for n = 8, a smectic A phase is observed, as shown in Fig. 10 and 11, respectively. The values of birefringence shown by CB7O.7.O7CB (Fig. 11) are significantly higher than those seen for the analogous tetramer having odd-membered outer spacers, CB6O.7.O6CB. This presumably reflects the high polarizability of the linear outer fragments of the tetramer. It is noteworthy that the value of $\Delta S_{NI}/R$ seen for CB7O.8.O7CB is double that of CB7O.7.O7CB. The pitch length measured in the N_{TB} phase shown by CB7O.7.O7CB was around 17 nm (Fig. 12), and was essentially the same as that seen for CB6O.7.O6CB[36] that combines a bent central fragment with two linear outer fragments.

The dependence of the nematic–isotropic transition temperatures, T_{NI}, on the length of the central flexible spacer in these four sets of tetramers is shown in Fig. 13. In order to make these comparisons meaningful, we should compare the

Table 3 Transition temperatures (°C), and associated scaled entropy changes ($\Delta S/R$) for the CB7O.O*m*O.O7CB series, and [•] indicates a monotropic transition. Data have been extracted from DSC traces measured on heating unless noted otherwise

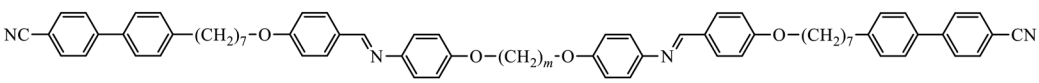

CB7O.O*m*O.O7CB

m	Cr		SmA		N		I
3	•	147 (5.65)	[•]	112[b]	•	253 (4.15)	•
4	•	166 (22.38)	[•]	138[b]	•	282 (6.12)	•
5	•	149 (9.21)	[•]	135[b]	•	255 (4.60)	•
6	•	169 (25.64)	[•]	134[b]	•	264 (6.47)	•
7	•	145 (24.40)	[•]	129[a] (0.01)	•	252 (4.90)	•
8	•	176 (20.18)	[•]	149[b]	•	260 (6.52)	•
9	•	143 (12.72)			•	245 (5.23)	•

[a] Data extracted from DSC cooling trace. [b] Transition temperature obtained using POM.

Table 4 Transition temperatures (°C), and associated scaled entropy changes ($\Delta S/R$) for the CB7O.*n*.O7CB series, and [•] indicates a monotropic transition. Data have been extracted from DSC traces measured on heating unless noted otherwise

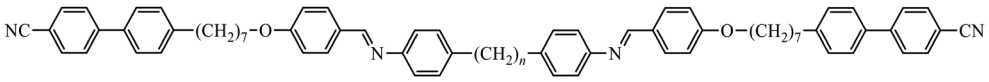

CB7O.*n*.O7CB

n	Cr		SmA		N_{TB}		N		I
7	•	145 (14.49)			[•]	132† (0.03)	•	225 (3.42)	•
8	•	165 (11.24)	[•]	155[a] (0.04)			•	257 (6.97)	•

[a] Data extracted from DSC cooling traces.

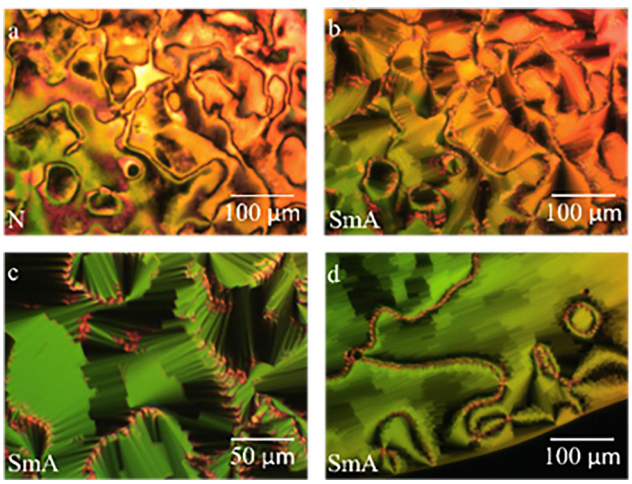

Fig. 8 (a) The schlieren texture of the nematic phase (T = 170 °C), and (b)–(d) the truncated fan-like texture of the smectic A phase (T = 130 °C) shown by CB7O.O5O.O7CB. Micrographs (a) and (b) correspond to the same region of the sample.

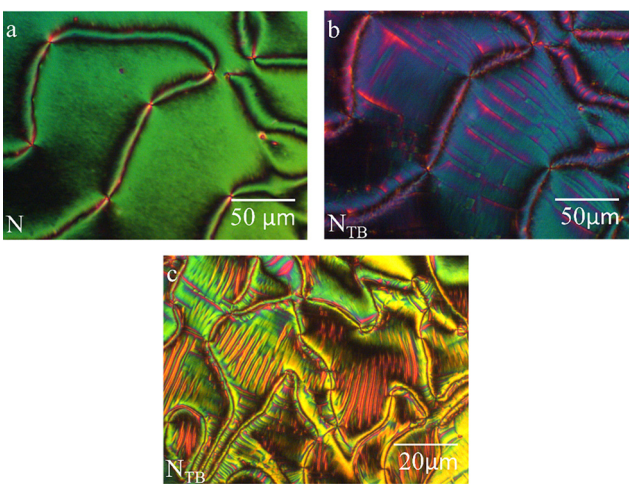

Fig. 9 (a) The schlieren texture of the nematic phase (T = 145 °C), and the texture of the twist-bend nematic phase at (b) T = 115 °C and (c) T = 102 °C shown by CB7O.7.O7CB. Micrographs (a) and (b) correspond to the same region of the sample.

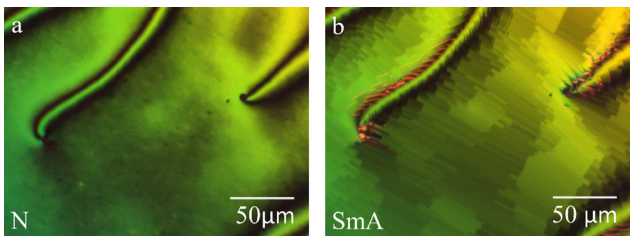

Fig. 10 (a) The texture of the nematic phase (T = 185 °C) and (b) the truncated fan texture of the smectic A phase (T = 146 °C) shown by CB7O.8.O7CB. The micrographs correspond to the same region of the sample.

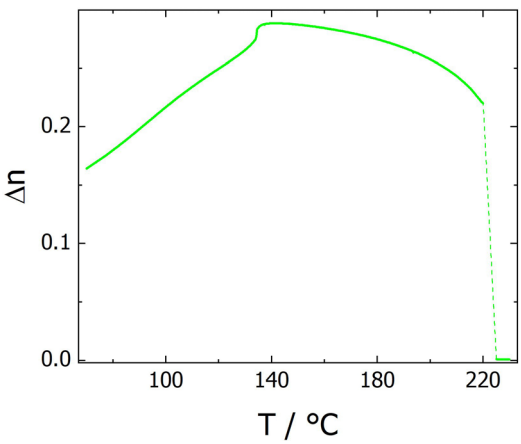

Fig. 11 The temperature dependence of the optical birefringence for CB7O.7.O7CB. Note that at the transition from isotropic liquid, the sample misalignment prevented recording reliable values.

properties of tetramers having the same number of atoms connecting the benzylideneaniline-based fragments such that the values of T_{NI} for members of the CB6O.O*m*O.O6CB and CB7O.O*m*O.O7CB series are compared to those of the corresponding CB6O.(n + 2).O6CB or CB7O.(n + 2).O7CB tetramers. For each set, the tetramers with an even-membered central spacer show higher values of T_{NI} than those having an odd-membered central spacer giving rise to an alternation on increasing spacer length (Fig. 13). This behaviour is most

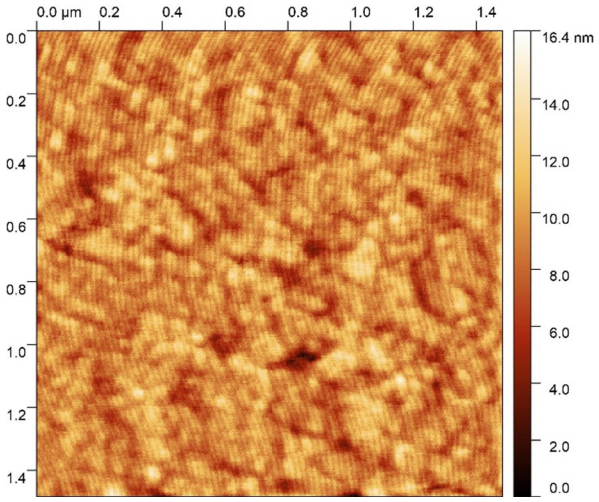

Fig. 12 AFM image of N_{TB} phase shown by CB7O.7.O76CB, and the stripe periodicity is 17 nm.

commonly accounted for in terms of how the central spacer controls the average shape of the tetramer. Thus, for an even-membered central spacer, the major axes of the two innermost mesogenic units are more or less parallel and that the fragment of the molecule is linear, whereas for an odd-membered spacer, the two mesogenic units are inclined at some angle with respect to each other giving a molecular bend (as is clear from the DFT energy-minimised structures illustrated in Fig. 14). The more linear conformations are more compatible with the nematic environment and give rise to the higher values of T_{NI}.

For any given value of p, *i.e.* the number of atoms connecting the two innermost mesogenic units, T_{NI} increases in the order:

CB6O.*n*.O6CB < CB6O.O*m*O.O6CB < CB7O.*n*.O7CB < CB7O.O*m*O.O7CB.

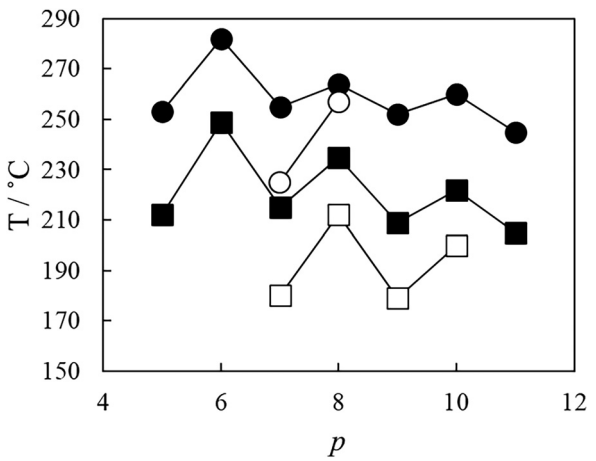

Fig. 13 The dependence of the nematic–isotropic transition temperature, T_{NI}, on the total number of atoms, p, connecting the benzylidene aniline-based units in the CB6O.O*m*O.O6CB (■), CB7O.O*m*O.O7CB (●), CB6O.*n*.O6CB (□) and CB7O.*n*.O7CB (○). For CB6O.O*m*O.O6CB and CB7O.O*m*O.O7CB, $p = (m + 2)$, and for CB6O.*n*.O6CB and CB7O.*n*.O7CB, $p = n$.

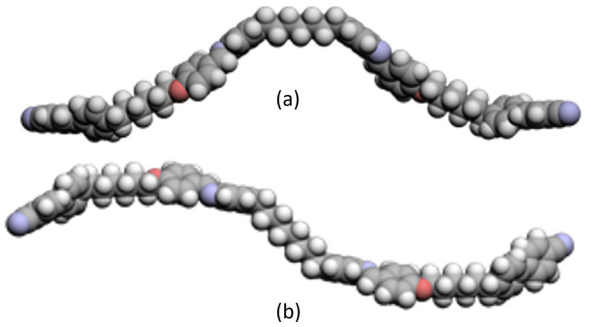

Fig. 14 Space-filling models (energy-minimised at the DFT level, see Experimental for details) comparing the shapes of (a) CB6O.7.O6CB and (b) CB6O.8.O6CB.

This trend is a combination of two effects. First, switching the link between the central spacer and the mesogenic units from an ether to a methylene group decreases the bond angle between the para axis of the mesogenic group and the first bond in the spacer from about 126.4° to 113.5°.[58–60] This difference means that the all-trans conformation of an ether-linked central fragment is more linear than that of the corresponding methylene-linked fragment and this greater shape anisotropy is expected to give rise to the higher transition temperatures. This change in shape is more pronounced for an odd-membered central spacer than for an even-membered central spacer and thus changing the parity of methylene-linked spacers gives rise to a larger alternation in T_{NI}, as shown in Fig. 13. The change in bond angle accounts for the relative values of T_{NI} for the tetramers with the same outer spacers but different central spacer. The second contributing effect is the change in shape associated with the parity of the two outer spacers. Again, an even spacer promotes a linear structural fragment, whereas an odd-membered spacer induces a molecular bend.

It is apparent through the data shown in Fig. 13 that the difference in T_{NI} on varying the parity of the outer spacers, for example, between the corresponding members of CB6O.O-*m*O.O6CB and CB7O.O*m*O.O7CB series, is greater than that seen on varying the central spacer, for example, within the CB7O.O*m*O.O7CB series. This has been observed for other tetrameric series[33–35] and is thought to suggest that orientationally, the four mesogenic units are not strongly correlated along the molecular length and thus varying the parity of the central spacer does not give rise to such a pronounced alternation in T_{NI} as seen for liquid crystal dimers.[26] Instead, the length and parity of the two outer spacers play a larger role in determining molecular shape. In this respect, the observation that the length and parity of the spacer having the major compositional fraction in the tetramer more strongly determine the transition temperatures reflects the behaviour of semi-flexible liquid crystal copolymers containing spacers of differing parities.[33] It is interesting to note that replacing the methylene links in CB6O.O8O.O6CB by ether links in CBO5O.O8O.O5OCB results in a higher value of T_{NI}, but the twist-bend nematic phase is no longer observed.[31] This again

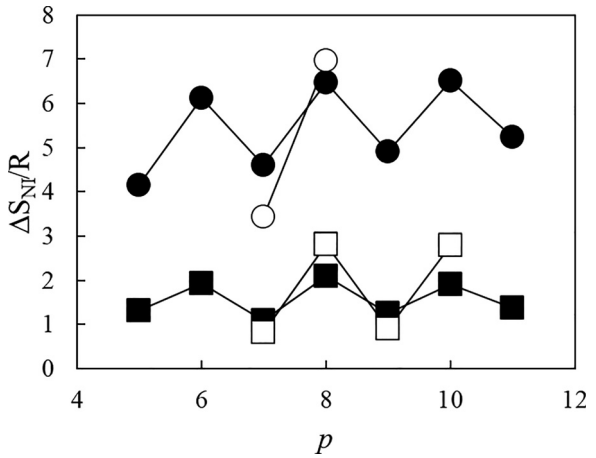

Fig. 15 The dependence of the scaled entropy change associated with the nematic–isotropic transition, $\Delta S_{NI}/R$, on the total number of atoms, p, connecting the benzylidene aniline-based units in the CB6O.O*m*O.O6CB (■), CB7O.O*m*O.O7CB (•), CB6O.*n*.O6CB (□) and CB7O.*n*.O7CB (○) series. For CB6O.O*m*O.O6CB and CB7O.O*m*O.O7CB, $p = (m + 2)$, and for CB6O.*n*.O6CB and CB7O.*n*.O7CB, $p = n$.

highlights the importance of shape in driving the formation of the N_{TB} phase.

The dependence of the scaled entropy change associated with the nematic–isotropic transition, $\Delta S_{NI}/R$, on the total number of atoms connecting the two inner mesogenic units for the tetramers is shown in Fig. 15. It is clear that within a given set, tetramers with even-membered central spacers exhibit higher values of $\Delta S_{NI}/R$ than those with odd-membered central spacers. This may be accounted for in terms of the conformational distribution of the spacer using a model developed to describe the behaviour of liquid crystal dimers. Thus, at the transition to the nematic from the isotropic phase, the synergy between conformational and orientational order ensures that bent conformers of an even-membered spacer are converted to linear forms, whereas the energy difference between linear and bent conformers for an odd-membered spacer is too large for this to happen.[61] This enhances the orientational order of the nematic phase exhibited by even-membered oligomers, and hence, these show higher values of $\Delta S_{NI}/R$. It is clear that the alternation seen in T_{NI} tends to attenuate on increasing the length of the central spacer (Fig. 13), whereas that shown by $\Delta S_{NI}/R$ does not (Fig. 15). This suggests that on increasing the length of the spacer, the number of its possible conformations increases and the shapes of the even- and odd-membered tetramers become more similar. Thus, the interaction strength parameters between the mesogenic units become more similar and the values of T_{NI} are less dependent on the parity of the spacer. There will still be a marked difference, however, in the conformational distribution of the spacers that underpins the alternation seen in $\Delta S_{NI}/R$ as the spacer length is increased.

It is striking in Fig. 15 that the values of $\Delta S_{NI}/R$ are several times larger for tetramers with even-membered outer spacers than for those with odd-membered outer spacers. Indeed, the values of $\Delta S_{NI}/R$ shown by CB7O.O*m*O.O7CB and CB7O.*n*.O7CB are almost without precedence for low mass mesogens, and to place these in context, for a conventional low molar mass nematogen consisting of molecules containing a single mesogenic core, $\Delta S_{NI}/R$ is typically around 0.3.[62] It has been suggested, however, that values of $\Delta S_{NI}/R$ should be scaled by the number of mesogenic units in an oligomer as routinely undertaken for polymeric systems.[62,63]

The differences in the values of $\Delta S_{NI}/R$ between the corresponding members of the CB7O.O*m*O.O7CB and CB6O.O*m*O.O6CB, and CB7O.*n*.O7CB and CB6O.*n*.O6CB series are larger than the differences within a series reinforcing the suggestion made earlier that orientationally the four mesogenic units are not strongly correlated along the molecular length, and the length and parity of the spacer having the major compositional fraction more strongly determines the transitional properties. It is also evident in Fig. 15 that the alternation seen in $\Delta S_{NI}/R$ for the methylene-linked tetramers is more pronounced than that seen for the ether-linked materials and this has been accounted for purely in terms of the change in geometry associated with the different bond angles between the para axis of the mesogenic group and the first bond in the spacer as described earlier.[58–60]

We now turn our attention to the phase behaviour of the studied tetramers, and the discussion will be predicated on the widely held view that molecular bend is a prerequisite for the observation of the twist-bend nematic phase. We have seen that the CB6O.O*m*O.O6CB and CB6O.*n*.O6CB series exhibit N_{TB} and N phases. The values of T_{NTBN} for the CB6O.O*m*O.O6CB tetramers alternate with the same manner as T_{NI} upon increasing the length of the central spacer, as shown in Fig. 13 and 16. Given that the alternation seen for T_{NI} was earlier interpreted in terms of molecular shape and that an even-membered central spacer enhanced shape anisotropy giving rise to a high value of

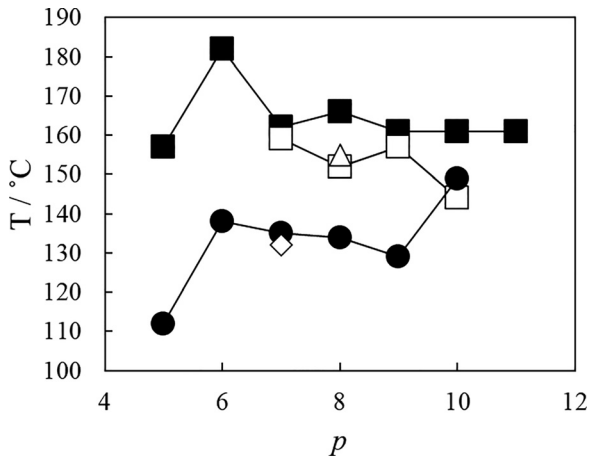

Fig. 16 The dependence of the transition temperatures on the total number of atoms, p, connecting the benzylidene aniline-base units in CB6O.O*m*O.O6CB (N_{TB}–N, ■), CB7O.O*m*O.O7CB (SmA–N, •), CB6O.*n*.O6CB (N_{TB}–N, □) and CB7O.*n*.O7CB (N_{TB}–N, ◊; SmA–N, △). For CB6O.O*m*O.O6CB and CB7O.O*m*O.O7CB, $p = (m + 2)$, and for CB6O.*n*.O6CB and CB7O.*n*.O7CB, $p = n$.

T_{NI}, it may appear counter-intuitive that the even-membered tetramers also exhibit the higher values of T_{NTBN}. We must remember, however, that enhancing the shape anisotropy facilitates the interactions between the mesogenic groups. These interactions compensate for the loss of entropy due to the additional local polar order in the N_{TB} phase,[64] counteracting the effect of the increase in bend angle moving from an odd- to an even-membered central spacer, and the stability of the N_{TB} phase increases. Increasing the length of the spacer dilutes the interactions between the mesogenic units as the volume fraction of alkyl chains increases, and T_{NTBN} would be expected to decrease to a greater extent for even-membered tetramers and this is observed as an attenuation in the odd–even effect, as shown in Fig. 16. The weaker alternation seen for the values of T_{NTBN} compared to T_{NI} on varying spacer length again suggests that the orientational correlation of the mesogenic units along the tetramer is not strong. Thus, the bent shapes of the outer fragments for the longer members of the CB6O.O*m*O.O6CB series are not strongly correlated by the inner spacer, irrespective of its parity and are rather similar as are their values of T_{NTBN} consistent with the view that the N_{TB}–N phase transition is predominantly shape driven. By contrast, an even member spacer will enhance the interactions between mesogenic units, and a stronger alternation is seen for T_{NI} on increasing *m*.

Surprisingly, the alternation seen for T_{NTBN} on varying the central spacer length for the CB6O.*n*.O6CB series is in the opposite sense to that observed for T_{NI}, as shown in Fig. 13 and 16. The values of T_{NTBN} shown by the odd-membered central spacers of the CB6O.*n*.O6CB and CB6O.O*m*O.O6CB series are very similar, whereas the even-members of the CB6O.*n*.O6CB series show significantly lower values of T_{NTBN} than their ether-linked counterparts. This strongly suggests that for the methylene-linked materials, the effect of the increase in the molecular bend angle on moving from an odd- to even-membered central spacer is not offset by enhanced interactions between the mesogenic units such that the shape change is the dominant effect and T_{NTBN} decreases. In oligomers containing cyanobiphenyl- and benzylideneaniline-based mesogenic groups, the mixed interaction between the unlike mesogenic units is known to be important in controlling phase behaviour[28,31,65,66] and it has been suggested to be an electrostatic quadrupolar interaction between groups with quadrupole moments which are opposite in sign.[67] This type of interaction will be stronger in the ether-linked than the methylene-linked tetramers, which accounts for the surprisingly high values of T_{NTBN} observed for the even members of the CB6O.O*m*O.O6CB series. We note, however, that the difference in these transition temperatures is rather small again, indicating that the central spacer does not strongly correlate the torsional fluctuations of the four mesogenic units.

The CB7O.O*m*O.O7CB series shows SmA and N phases. This reflects that the outer spacers are even-membered and hence, the molecule is now more linear. For m = 4–7, T_{SmAN} decreases monotonically indicating again that the central spacer does not control molecular shape. The sharp increase in T_{SmAN} passing from m = 3 to 4, and again between m = 7 and 8 is presumably related to specific packing issues within the smectic phase that will depend on the relative lengths of the spacers but it would be unwise to speculate further on this matter without the knowledge of the smectic periodicities. CB7O.8.O7CB also exhibits a smectic A-nematic transition, and T_{SmAN} is higher than that seen for CB7O.O6O.O7CB. This observation may be accounted for in terms of the bond angle between the *para* axis of the mesogenic group and the first bond in the spacer and how this affects the molecular geometry as described earlier. By contrast, CB7O.7.O7CB shows an N_{TB}–N transition, indicating that the bend angle associated with the central fragment is now sufficiently small to drive the formation of the N_{TB} phase even though the two outer fragments are linear. Here we have a rare example of the minor compositional fraction in the tetramer driving the phase behaviour.

Finally, we consider the behaviour of CB6O.6O.O6CB and CB7O.6O.O7CB, and their transitional properties are listed in Table 5. CB6O.6O.O6CB shows N_{TB} and N phases as described previously.[36] The helical pitch length measured in the N_{TB} phase is around 35 nm, significantly larger than that seen for dimers but comparable to that shown by CB6O.O5O.O6CB described earlier. In contrast, CB7O.6O.O7CB exhibits two smectic phases and the nematic phase (Fig. 17). A characteristic nematic optical texture was observed which on cooling gave a focal conic fan texture indicative of a smectic A phase. On

Table 5 Transition temperatures (°C), and associated scaled entropy changes ($\Delta S/R$) for the CB*n*O.6O.O*n*CB tetramers. [•] indicates a monotropic transition. Data have been extracted from DSC traces measured on heating unless noted otherwise

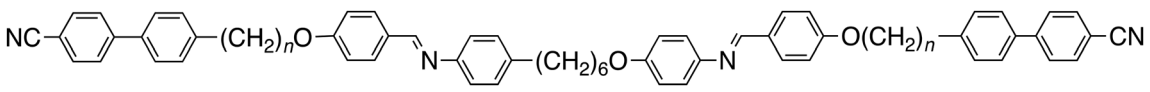

CB*n*O.6O.O*n*CB

n	Cr		Sm		SmA		N_{TB}		N		I
6	•	151 (8.62)					•	158 (0.36)	•	195 (1.01)	•
7	•	128 (18.29)	[•]	75[a]	[•]	126[a] (0.07)			•	242 (4.07)	•

[a] Data extracted from the DSC cooling trace.

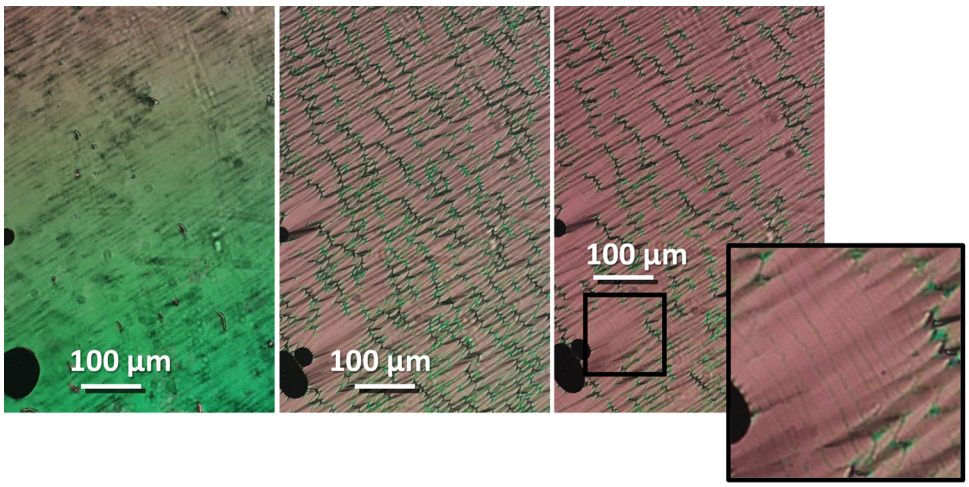

Fig. 17 The optical textures shown by CB7O.6O.O7CB: (left) nematic phase (T = 152 °C); (centre) smectic A phase (T = 89 °C); (right) smectic phase showing (inset) lines crossing the backs of the fans (T = 69 °C).

further cooling, faint lines developed across the backs of the fans suggest an increase in the in-plane ordering of the molecules. The monotropic nature of the smectic phase precluded its further characterisation using X-ray diffraction.

CB6O.6O.O6CB may be considered as a nonsymmetric tetramer derived from CB6O.7.O6CB and CB6O.O5O.O6CB. As we have seen, the nature of the link between the central spacer and mesogenic units plays an important role in determining the shape of that fragment. Specifically, the heptyl spacer will give rise to the most bent fragment and the O5O spacer the least bent with the 6O spacer inducing an intermediate bend angle. On this basis, it would be expected that the transition temperatures of the 6O tetramer would be intermediate between the other two as indeed they are. Furthermore, these three dimers show N_{TB} and N phases. This indicates that the average bend angle of the structural fragments comprising these tetramers falls within the range that supports the formation of the N_{TB} phase[64] bearing in mind our earlier comment that the central spacer plays a limited role in correlating the torsional fluctuations of the outer fragments.

A similar comparison of CB7O.6O.O7CB with CB7O.O5O.O7CB and CB7O.7.O7CB reveals somewhat different behaviour. All three exhibit a nematic phase and the value of T_{NI} shown by the hexyloxy-linked tetramer lies between those of the other two tetramers as would be expected. As we have seen, however, the heptyl-linked tetramer shows a N_{TB} phase, whereas the O5O and 6O-based tetramers exhibit smectic behaviour. The value of T_{NTBN} shown by the heptyl linked tetramer lies between the values of T_{SmAN} shown by the other two. This reinforces our comment made earlier that CB7O.7.O7CB is unusual in that the fragment having the minor compositional fraction determines the phase behaviour. This reflects the greater bend angle associated with the heptyl spacer that drives the formation of the N_{TB} phase.

We note that the entropy change associated with the SmA–N transition, $\Delta S_{SmAN}/R$, could be measured for just three tetramers, CB7O.6O.O7CB, CB7O.O7O.O7CB and CB7O.8.O7CB, and for each, the value was very small. These values are in accordance with McMillan theory[68] that predicts that the strength of the SmA–N transition, as reflected by $\Delta S_{SmAN}/R$, decreases as the nematic range increases which may be described using the McMillan parameter that is defined as the ratio of the transition temperatures, T_{SmAN}/T_{NI}. For these tetramers, the McMillan parameters are small ranging between 0.77 and 0.81 and hence the associated values of $\Delta S_{SmAN}/R$ are expected to be small. Indeed, McMillan theory predicts that $\Delta S_{SmAN}/R$ will continue to decrease as T_{SmAN}/T_{NI} decreases until a tricritical point is reached at which the transition becomes second order. The entropy change associated with the N_{TB}–N transition behaves in, at least qualitatively, the same way such that the closer the ratio T_{NTBN}/T_{NI} is to one, the stronger the N_{TB}–N transition becomes. This is in accord with the predictions made by a Landau model developed to describe the N_{TB}–N transition.[69]

Finally, Table 6 summaries the values of the helical pitch length measured in the N_{TB} phase for a selection of these tetramers and those studied in our previous work.[36] As described earlier, such values of pitch are obtained from AFM measurements of samples quenched to room temperature in the N_{TB} phase and as such, no temperature dependence of pitch can be concluded by these data. The pitch length of CB6O.7.O6CB was measured by AFM and additionally by resonant soft X-ray scattering (RSoXS);[36] both techniques showed a

Table 6 A summary of the pitch lengths measured in the N_{TB} phase for the tetramers, and the structure description in terms of bent (B) and linear (L) fragments

Tetramer	Pitch length/nm	Structure	Ref.
CB6O.O5O.O6CB	30	BBB	This work
CB6O.6O.O6CB	35	BBB	This work
CB6O.7.O6CB	7	BBB	36
CB7O.7.O7CB	17	LBL	This work
CBO6O.7.O6OCB	17	LBL	36
CB6O.8.O6CB	12	BLB	36

good agreement in the magnitude of the pitch and the latter allowed the temperature dependence to be observed, one much weaker than that observed for twist-bend nematic dimers.

From this limited dataset, it is difficult to determine any regular relationship between the molecular structure and pitch length for twist-bend nematic tetramers. For structures with BBB – that is, bent internal and external spacers – we can observe a significantly large increase in pitch upon moving from a purely alkyl internal spacer to those with at least one ether-linkage, thus the nature of the internal linkage appears to play a crucial role. The short pitch of CB6O.7.6OCB is more similar to that observed in dimers, perhaps because this tetramer looks very similar to two dimers in terms of the bend angles. As the internal junction becomes more linear, this will strongly influence the relative direction of the terminal mesogenic cores and consequently the pitch becomes much longer, but the physical significance of this observation is not yet clear and it will be the subject of future investigation.

Conclusions

Liquid crystal tetramers consist of molecules containing four mesogenic units linked by three spacers and as such may be thought of in terms of three structural fragments defined by the spacers, the shapes of which are largely governed by the parity of the respective spacer. Thus, an odd membered spacer gives a bent fragment, whereas an even-membered spacer yields a linear fragment. The bend angle associated with the spacer may be tuned by changing the nature of the chemical links between the spacer and mesogenic units. A spacer connected by ether links gives rise to the largest bend angle, and a spacer connected by two methylene links gives rise to the smallest bend angle. Here, we have considered three types of spacers: linked by two ether groups (O*m*O), by two methylene groups (*n*) and by a methylene and an ether group (*n*O). In each group of tetramers studied, the outer spacers are held constant, and the central spacer is varied. The magnitudes of the alternation in the values of T_{NI} and $\Delta S_{NI}/R$ seen on varying the length and parity of the central spacer suggest that the torsional fluctuations of the four mesogenic units are not strongly correlated along the molecule. Changes in the transitional properties between these groups may be interpreted by the changes in shape associated with changing the linking groups. We suggest, however, that geometrical factors alone cannot account for the surprising inversion in the sense of the alternation in T_{NTBN} on switching between O*m*O and *n* spacers and instead, how this change affects the interactions between the unlike mesogenic groups must also be taken into consideration. In general, the phase behaviour of the tetramers is determined by the parity of the spacer having the larger compositional fraction. Thus, tetramers with odd-membered outer spacers exhibit the N_{TB} phase, whereas those with two even-membered spacers exhibit the SmA phase. The sole exception to this is a heptyl-linked tetramer and this is suggested to reflect the highly bent nature of this internal spacer. The nature of the internal spacer appears to have the most significant effect on the pitch length; tetramers with methylene–ether or di-ether-links in the central spacer have markedly longer pitch lengths (~30–35 nm) than their methylene-linked equivalent (~10 nm), though a larger pool of materials is now required to study this phenomenon further. This study has shown that the phase behaviour and transitional properties of liquid crystal tetramers may be tailored in a rational manner by varying the nature of the flexible spacers, although it is clear that we still have much to learn about these fascinating achiral materials that spontaneously form chiral structures.

Conflicts of interest

There are no conflicts to declare.

Data availability

The data supporting this article have been included as part of the supplementary information (SI). Supplementary information is available. See DOI: https://doi.org/10.1039/d5tc03351a.

Acknowledgements

The authors would like to acknowledge the immense contributions to this project, as well as past, ongoing present, and future work by Professor CT Imrie, who passed away suddenly in January 2025. MMM, EG and DP acknowledge the project FerroFluid, EIG Concert Japan, 9th Joint call (EIG CONCERT-JAPAN/9/89/FerroFluid/2023.

References

1 A. Guijarro and M. Yus, The Origin of Chirality in the Molecules of Life: A Revision from Awareness to the Current Theories and Perspectives of This Unsolved Problem.
2 M. Cestari, *et al.*, Phase behavior and properties of the liquid-crystal dimer 1,7-bis(4-cyanobiphenyl-4-yl) heptane: A twist-bend nematic liquid crystal, *Phys. Rev. E: Stat., Nonlinear, Soft Matter Phys.*, 2011, **84**, 031704.
3 V. Borshch, *et al.*, Nematic twist-bend phase with nanoscale modulation of molecular orientation, *Nat. Commun.*, 2013, **4**, 2635.
4 D. Chen, *et al.*, Chiral heliconical ground state of nanoscale pitch in a nematic liquid crystal of achiral molecular dimers, *Proc. Natl. Acad. Sci.*, 2013, **110**, 15931–15936.
5 I. Dozov, On the spontaneous symmetry breaking in the mesophases of achiral banana-shaped molecules, *EPL*, 2001, **56**, 247.
6 R. Walker, D. Pociecha, J. M. D. Storey, E. Gorecka and C. T. Imrie, The Chiral Twist-Bend Nematic Phase (N*TB), *Chem. – Eur. J.*, 2019, **25**, 13329–13335.
7 R. Walker, *et al.*, Intrinsically Chiral Twist-Bend Nematogens: Interplay of Molecular and Structural Chirality in the NTB Phase, *Chem. Phys. Chem.*, 2023, **24**, e202300105.

8 J. P. Abberley, *et al.*, Heliconical smectic phases formed by achiral molecules, *Nat. Commun.*, 2018, **9**, 228.
9 M. Salamończyk, *et al.*, Multi-level chirality in liquid crystals formed by achiral molecules, *Nat. Commun.*, 2019, **10**, 1922.
10 D. Pociecha, *et al.*, Photonic Bandgap in Achiral Liquid Crystals—A Twist on a Twist, *Adv. Mater.*, 2021, **33**, 2103288.
11 Y. Arakawa, T. Shiba and K. Igawa, Selenium-linked cyanobiphenyl-based liquid crystal dimers: the effects of chalcogen linkage and spacer length on the twist-bend nematic phase, *Liq. Cryst.*, 2024, **51**, 1506–1522.
12 A. Ožegović, *et al.*, The Interplay of Spacer Chirality and Parity in Mesogenic Dimers, *Chem. Phys. Chem.*, 2024, **25**, e202400065.
13 A. F. Alshammari, *et al.*, Heliconical nematic and smectic phases: the synthesis and characterisation of the CB4O.m and CB8O.m series, *Liq. Cryst.*, 2024, **51**, 2300–2312.
14 Y. Arakawa, K. Horita and K. Igawa, Phase behaviour of ester-linked cyanobiphenyl dimers and fluorinated analogues: the direct isotropic to twist-bend nematic phase transition, *Liq. Cryst.*, 2023, **50**, 2216–2228.
15 E. Cruickshank, *et al.*, The influence of the imine bond direction on the phase behaviour of symmetric and non-symmetric liquid crystal dimers, *J. Mol. Liq.*, 2023, **391**, 123226.
16 D. A. Paterson, R. Walker, J. M. D. Storey and C. T. Imrie, Molecular structure and the twist-bend nematic phase: the role of spacer length in liquid crystal dimers, *Liq. Cryst.*, 2023, **50**, 725–736.
17 D. Wang, *et al.*, Facile Synthesis of Liquid Crystal Dimers Bridged with a Phosphonic Group, *Chem. – Eur. J.*, 2022, **28**, e202202146.
18 Y. Arakawa, Y. Arai, K. Horita, K. Komatsu and H. Tsuji, Twist–Bend Nematic Phase Behavior of Cyanobiphenyl-Based Dimers with Propane, Ethoxy, and Ethylthio Spacers, *Crystals*, 2022, **12**, 1734.
19 E. Cruickshank, *et al.*, Helical phases assembled from achiral molecules: Twist-bend nematic and helical filamentary B4 phases formed by mesogenic dimers, *J. Mol. Liq.*, 2022, **346**, 118180.
20 A. F. Alshammari, *et al.*, New patterns of twist-bend liquid crystal phase behaviour: the synthesis and characterisation of the 1-(4-cyanobiphenyl-4′-yl)-10-(4-alkylaniline-benzylidene-4′-oxy)decanes (CB10O·m), *Soft Matter*, 2022, **18**, 4679–4688.
21 D. A. Paterson, *et al.*, Azobenzene-based liquid crystal dimers and the twist-bend nematic phase, *Liq. Cryst.*, 2017, **44**, 2060–2078.
22 E. Cruickshank, *et al.*, Cyanobiphenyl-based liquid crystal dimers and the twist-bend nematic phase: on the role played by the length and parity of the spacer, *Liq. Cryst.*, 2024, **51**, 1446–1470.
23 C. J. Gibb, J. M. D. Storey and C. T. Imrie, Molecular curvature and the twist-bend liquid crystal phases: the effect of the spacer, *Liq. Cryst.*, 2024, **51**, 1956–1963.
24 C. J. Gibb, *et al.*, Liquid Crystal Dimers and the Twist-Bend Phases: Non-Symmetric Dimers Consisting of Mesogenic Units of Differing Lengths, *Chem. Phys. Chem.*, 2024, **25**, e202300848.
25 C. T. Imrie and P. A. Henderson, Liquid crystal dimers and higher oligomers: between monomers and polymers, *Chem. Soc. Rev.*, 2007, **36**, 2096–2124.
26 C. T. Imrie, P. A. Henderson and G.-Y. Yeap, Liquid crystal oligomers: going beyond dimers, *Liq. Cryst.*, 2009, **36**, 755–777.
27 N. Tufaha, C. J. Gibb, J. M. D. Storey and C. T. Imrie, Can even-membered liquid crystal dimers exhibit the twist-bend nematic phase? The preparation and properties of disulphide and thioether linked dimers, *Liq. Cryst.*, 2023, **50**, 1362–1374.
28 C. T. Imrie, P. A. Henderson and J. M. Seddon, Non-symmetric liquid crystal trimers. The first example of a triply-intercalated alternating smectic C phase, *J. Mater. Chem.*, 2004, **14**, 2486–2488.
29 P. A. Henderson and C. T. Imrie, Non-symmetric liquid crystal trimers, *Liq. Cryst.*, 2005, **32**, 673–682.
30 T. Donaldson, P. A. Henderson, M. F. Achard and C. T. Imrie, Non-symmetric chiral liquid crystal trimers, *Liq. Cryst.*, 2011, **38**, 1331–1339.
31 C. T. Imrie, *et al.*, Liquid crystal tetramers, *J. Mater. Chem.*, 1999, **9**, 2321–2325.
32 P. A. Henderson, R. T. Inkster, J. M. Seddon and C. T. Imrie, Highly non-linear liquid crystal tetramers, *J. Mater. Chem.*, 2001, **11**, 2722–2731.
33 P. A. Henderson and C. T. Imrie, Semiflexible Liquid Crystalline Tetramers as Models of Structurally Analogous Copolymers, *Macromolecules*, 2005, **38**, 3307–3311.
34 P. A. Henderson and C. T. Imrie, Liquid crystal tetramers: influence of molecular shape on liquid crystal behaviour, *Liq. Cryst.*, 2005, **32**, 1531–1541.
35 T. Donaldson, P. A. Henderson, M. F. Achard and C. T. Imrie, Chiral liquid crystal tetramers, *J. Mater. Chem.*, 2011, **21**, 10935–10941.
36 M. M. Majewska, *et al.*, Controlling spontaneous chirality in achiral materials: liquid crystal oligomers and the heliconical twist-bend nematic phase, *Chem. Commun.*, 2022, **58**, 5285–5288.
37 R. J. Mandle and J. W. Goodby, A Liquid Crystalline Oligomer Exhibiting Nematic and Twist-Bend Nematic Mesophases, *Chem. Phys. Chem.*, 2016, **17**, 967–970.
38 R. J. Mandle, M. P. Stevens and J. W. Goodby, Developments in liquid-crystalline dimers and oligomers, *Liq. Cryst.*, 2017, **44**, 2046–2059.
39 R. J. Mandle, The dependency of twist-bend nematic liquid crystals on molecular structure: a progression from dimers to trimers, oligomers and polymers, *Soft Matter*, 2016, **12**, 7883–7901.
40 M. R. Tuchband, *et al.*, Distinct differences in the nanoscale behaviors of the twist–bend liquid crystal phase of a flexible linear trimer and homologous dimer, *Proc. Natl. Acad. Sci.*, 2019, **116**, 10698–10704.
41 R. J. Mandle and J. W. Goodby, A Nanohelicoidal Nematic Liquid Crystal Formed by a Non-Linear Duplexed Hexamer, *Angew. Chem., Int. Ed.*, 2018, **57**, 7096–7100.
42 Y. Arakawa, K. Komatsu, S. Inui and H. Tsuji, Thioether-linked liquid crystal dimers and trimers: The twist-bend nematic phase, *J. Mol. Struct.*, 2020, **1199**, 126913.

43 R. Walker, *et al.*, Twist-Bend Nematogenic Supramolecular Dimers and Trimers Formed by Hydrogen Bonding, *Crystals*, 2020, **10**, 175.
44 A. Al-Janabi, R. J. Mandle and J. W. Goodby, Isomeric trimesogens exhibiting modulated nematic mesophases, *RSC Adv.*, 2017, **7**, 47235–47242.
45 Y. Arakawa, K. Komatsu, Y. Ishida, T. Shiba and H. Tsuji, Thioether-Linked Liquid Crystal Trimers: Odd–Even Effects of Spacers and the Influence of Thioether Bonds on Phase Behavior, *Materials*, 2022, **15**, 1709.
46 Y. Arakawa, K. Komatsu and H. Tsuji, 2,7-substituted fluorenone-based liquid crystal trimers: twist-bend nematic phase induced by outer thioether linkage, *Phase Transitions*, 2022, **95**, 331–339.
47 Y. Arakawa, K. Komatsu, T. Shiba and H. Tsuji, Phase behaviors of classic liquid crystal dimers and trimers: Alternate induction of smectic and twist-bend nematic phases depending on spacer parity for liquid crystal trimers, *J. Mol. Liq.*, 2021, **326**, 115319.
48 G. J. Strachan, *et al.*, Liquid crystal trimers containing secondary amide groups, *Liq. Cryst.*, 2024, **51**, 2059–2068.
49 J. Xiang, *et al.*, Electrically Tunable Selective Reflection of Light from Ultraviolet to Visible and Infrared by Heliconical Cholesterics, *Adv. Mater.*, 2015, **27**, 3014–3018.
50 J. Xiang, *et al.*, Electrically tunable laser based on oblique heliconical cholesteric liquid crystal, *Proc. Natl. Acad. Sci.*, 2016, **113**, 12925–12928.
51 S. M. Salili, *et al.*, Magnetically tunable selective reflection of light by heliconical cholesterics, *Phys. Rev. E*, 2016, **94**, 042705.
52 G. Nava, *et al.*, Heliconical cholesteric liquid crystals as electrically tunable optical filters in notch and bandpass configurations, *Liq. Cryst.*, 2021, **48**, 1534–1543.
53 S. Aya, *et al.*, Fast-and-Giant Photorheological Effect in a Liquid Crystal Dimer, *Adv. Mater. Interfaces*, 2019, **6**, 1802032.
54 M. J. Frisch *et al.*, *Gaussian 09 Revision D.01*, 2016.
55 M. Tarini, P. Cignoni and C. Montani, Ambient Occlusion and Edge Cueing for Enhancing Real Time Molecular Visualization, *IEEE Trans. Vis. Comput. Graph.*, 2006, **12**, 1237–1244.
56 D. A. Paterson, *et al.*, Understanding the twist-bend nematic phase: the characterisation of 1-(4-cyanobiphenyl-4′-yloxy)-6-(4-cyanobiphenyl-4′-yl)hexane (CB6OCB) and comparison with CB7CB, *Soft Matter*, 2016, **12**, 6827–6840.
57 Y. Arakawa, *et al.*, Birefringence and photoluminescence properties of diphenylacetylene-based liquid crystal dimers, *New J. Chem.*, 2020, **44**, 17531–17541.
58 A. P. J. Emerson and G. R. Luckhurst, On the relative propensities of ether and methylene linkages for liquid crystal formation in calamitics, *Liq. Cryst.*, 1991, **10**, 861–868.
59 A. Ferrarini, G. R. Luckhurst, P. L. Nordio and S. J. Roskilly, Understanding the unusual transitional behaviour of liquid crystal dimers, *Chem. Phys. Lett.*, 1993, **214**, 409–417.
60 A. Ferrarini, G. R. Luckhurst, P. L. Nordio and S. J. Roskilly, Prediction of the transitional properties of liquid crystal dimers. A molecular field calculation based on the surface tensor parametrization, *J. Chem. Phys.*, 1994, **100**, 1460–1469.
61 G. R. Luckhurst, Liquid crystals: a chemical physicist's view, *Liq. Cryst.*, 2005, **32**, 1335–1364.
62 C. T. Imrie and G. R. Luckhurst, Liquid crystal trimers. The synthesis and characterisation of the 4,4′-bis[ω-(4-cyanobiphenyl-4′-yloxy)alkoxy]biphenyls, *J. Mater. Chem.*, 1998, **8**, 1339–1343.
63 P. Henderson, A. Cook and C. Imrie, Oligomeric liquid crystals: From monomers to trimers, *Liq. Cryst.*, 2004, **31**, 1427–1434.
64 C. Greco, G. R. Luckhurst and A. Ferrarini, Molecular geometry, twist-bend nematic phase and unconventional elasticity: a generalised Maier–Saupe theory, *Soft Matter*, 2014, **10**, 9318–9323.
65 C. T. Imrie, Non-symmetric liquid crystal dimers: how to make molecules intercalate, *Liq. Cryst.*, 2006, **33**, 1449–1485.
66 D. A. Paterson, *et al.*, The role of a terminal chain in promoting the twist-bend nematic phase: the synthesis and characterisation of the 1-(4-cyanobiphenyl-4′-yl)-6-(4-alkyloxyanilinebenzylidene-4′-oxy)hexanes, *Liq. Cryst.*, 2018, **45**, 2341–2351.
67 A. E. Blatch, I. D. Fletcher and G. R. Luckhurst, The intercalated smectic A phase. The liquid crystal properties of the α-(4-cyanobiphenyl-4′-yloxy)-ω)-(4-alkyloxycinnamoate)alkanes, *Liquid Crystals*, 1995, **18**, 801–809.
68 W. L. McMillan, Simple Molecular Model for the Smectic A Phase of Liquid Crystals, *Phys. Rev. A*, 1971, **4**, 1238–1246.
69 D. O. López, *et al.*, Miscibility studies of two twist-bend nematic liquid crystal dimers with different average molecular curvatures. A comparison between experimental data and predictions of a Landau mean-field theory for the NTB–N phase transition, *Phys. Chem. Chem. Phys.*, 2016, **18**, 4394–4404.